Beam test of the silicon timing for use in calorimetry.

A. Apresyan[1], G. Bolla[2], H. Kim[3], S. Los[2], C. Pena[1], F. Presutti[1], E. Ramberg[2], A. Ronzhin[2], M. Spiropulu[1], and S. Xie[1]

[1] *California Institute of Technology, Pasadena, CA, USA*
[2] *Fermi National Accelerator Laboratory, Batavia, IL, USA*
[3] *University of Chicago, Chicago, IL, USA*

Abstract

The high luminosity upgrade of the Large Hadron Collider (HL-LHC) at CERN is expected to provide instantaneous luminosities of 5×10^{34} cm^{-2} s^{-1}. Collision at the high luminosity has shorter bunch spacing and more pileup [PU] events in the complex luminous regions. Precision timing allows extend calorimetric measurements into high density environment. We performed some study of the possible options to improve timing for calorimetry [1–4]. CMS calorimetry upgrade based on silicon as sensitive layer is another upgrade option [5]. Signal response of silicon detectors could be about few ns with rise time of ∼1 ns. 8000 e-h pairs produced in silicon per 100 μm, which is much higher than silicon noise . These properties with relatively high radiation hardness [6] allow to use silicon in calorimetric detectors. In this article we present results of timing study of silicon produced by Hamamatsu [7].

1 Introduction

One way to mitigate the pileup confusion effects, complementary to precision tracking methods, is to perform a time of arrival measurement associated with a particular layer of the calorimeter, allowing for a time assignment for both charged particles and photons. Such a measurement with a precision of about 20-30 ps, when unambiguously associated to the corresponding energy measurement, will significantly reduce the inclusion of pileup particles in the reconstruction of the event of interest, given that the spread in collision time of the pileup interactions is approximately 200 ps. The association of the time measurement with the energy measurement is crucial, and leads to a prototype design that calls for the time and energy measurements to be performed in the same active detector element. It is in this context that we studied the possibility of measuring the time of arrival of the particles with a calorimetric device when using silicon as sensitive element. The paper is organized as follows. The general silicon timing properties are described and bench test results of the used silicon described in Section 2. Test beam setup are presented in Section 3, and the results of the silicon test are presented in Section 4. Sections 5 and 6 are devoted to discussion and conclusion, respectively.

2 Silicon timing. Bench test of used silicon

Few factors determine the timing response of silicon detectors. One of them defines time constant and depends on series resistance of the silicon, load resistance and terminal capacitance. The other are due to silicon intrinsic properties: the silicon thickness, the carriers velocity and its

collection time, dependent on depletion voltage and type of the carriers. The carriers drift time in fully depleted silicon determines the carriers collection time. This time determines the silicon time response in case of small time constant, but the response could be mostly dependent on time constant for silicon with large capacitance.We used for our test the silicon, produced by Hamamatsu [7]. The thickness of the silicon is 325 μm. The transverse size of the silicon is 6x6 mm^2. The negative bias voltage was applied to p-side of the silicon. The dependence of the diode capacitance on the bias voltage is presented in Fig. 1. The junction capacitance depends on the area of p-layer and the thickness of the depletion layer which increased with inverse bias voltage. When charged particle pass through the silicon the produced electrons collected on the opposite (to p-side) n-side of the silicon and forms the output signal. The electrical schematics of the silicon diode and capacitance dependence on bias voltage presented in Fig. 1.

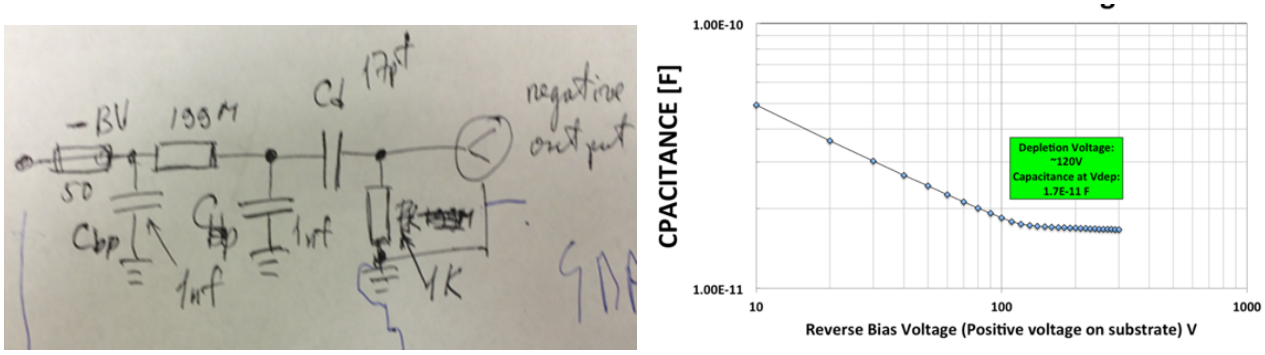

Figure 1: Electrical schematics of the silicon diode (left) and it capacitance in dependence on bias voltage (right).

The silicon box and bench test setup presented in Fig. 2. Measurements were performed at SiDet facility of Fermilab. The sensitivity of the silicon diode to light was tested to check it functionality.

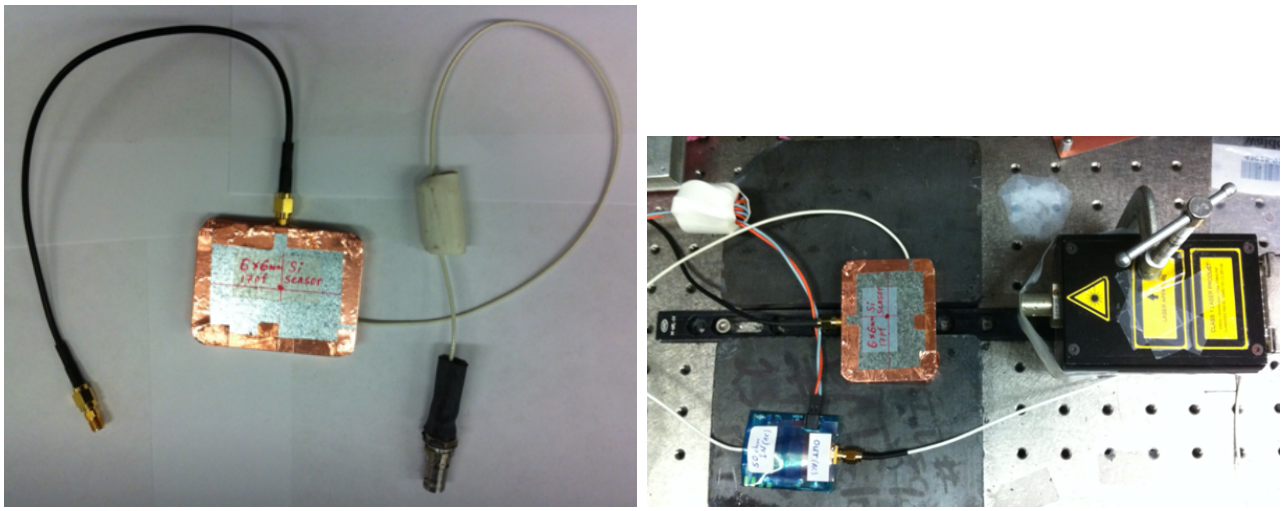

Figure 2: External view of the box with silicon diode and PC board inside (left) and bench test setup (right).

The silicon diode was placed in the metal box. The HV was applied to the PC board by the cable terminated by HSV connector. The silicon diode output signal was taken out by using the SMA connector attached to the box. Dark current dependence on bias voltage was tested. The maximum value of the current at -500 V of the bias was less of 1nA. (we had not in hands picoampermeter to measure the current).

3 Test beam setup and results of the silicon test

The test beam measurements were performed in FTBF. The main parts of the setup are well described in Refs. [1–4]. For the measurement with silicon it was slightly modified as shown in Fig. 3.

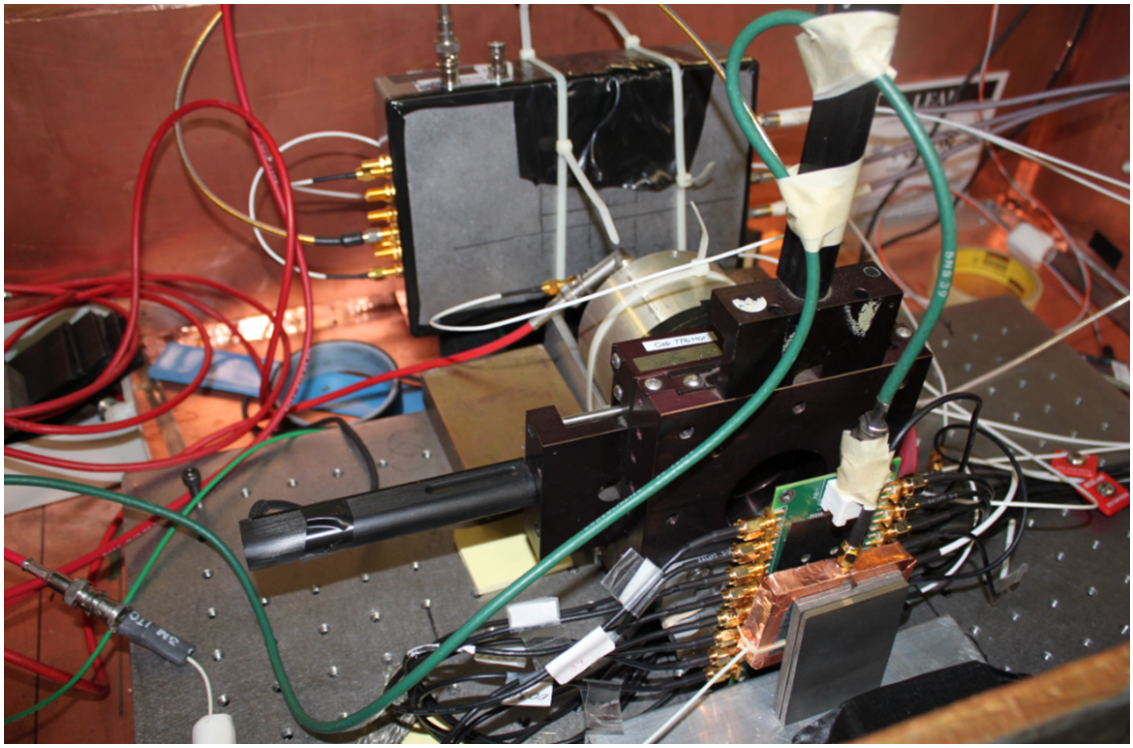

Figure 3: Test beam setup.

The test beam setup is shown in Fig. 3. The silicon detector was placed inside of the metal box. The absorber (W or Pb) was placed upstream for measurements with electron beam. We have not used absorber in measurements with 120 GeV protons. Other detectors which shown in the Fig. 3 were tested simultaneously. The setup contains a data acquisition (DAQ) system based on CAEN V1742 5 Gs/s digitizer [8], HV power supplies, and equipment to monitor and control test beam parameters. The dark box was located on a moving table allowing us to change the box position both in the horizontal and vertical direction in the range of 300 mm in X and Y with an accuracy better than 0.5 mm. Event selection and analysis was described in detail in Ref. [2]. The trigger was based on a scintillation counter with 1.8 x 2 mm2 transverse size. **DO WE NEED TO TALK ABOUT THESE The three detectors (4x4 Hamamatsu MPPC matrix [16], Photek 240 timing reference MCP-PMT and 6x6 cm2 LAPD [17])** were placed in line downstream of the tested silicon. The silicon detector was positioned on an X-Y moving stage, which allowed movement in both X and Y directions by ±15mm. The stage was operated remotely from the test beam control room. It was possible to align the silicon detector with 10 μm accuracy in both X and Y directions. The tungsten absorber material was used to initiate an electromagnetic shower when high energy electrons pass through. Signals from the detectors and the Cherenkov counter used for electron identification were split by high frequency Mini-Circuits ZFRSC-42-S splitters (4.2 GHz BW). The outputs were connected to CAEN V1742 digitizer, which allowed to hook up 32 channels for the measurements. The schematic of the similar readout (with DRS4) is described in detail in [1].

4 Test Beam Measurements and Results

Measurements were performed using the secondary beam at the FTBF, which provides a beam of electrons and pions. Beam energies ranging from 4 GeV/c^2 to 32 GeV/c^2 were used, for which the electron purity ranges between 70% at the lowest energy to about 10% at the highest energy. Stacks of tungsten plates with different thicknesses were placed immediately upstream of the silicon device in order to measure the response along the longitudinal direction of the electromagnetic shower. The transverse size of the tungsten plates allowed us to fully cover the transverse size of the silicon device. The signals from the silicon sensor and the Photek MCP-PMT are read out and digitized by the V1742 digitizer, and example signal waveforms are shown in Fig. 4.

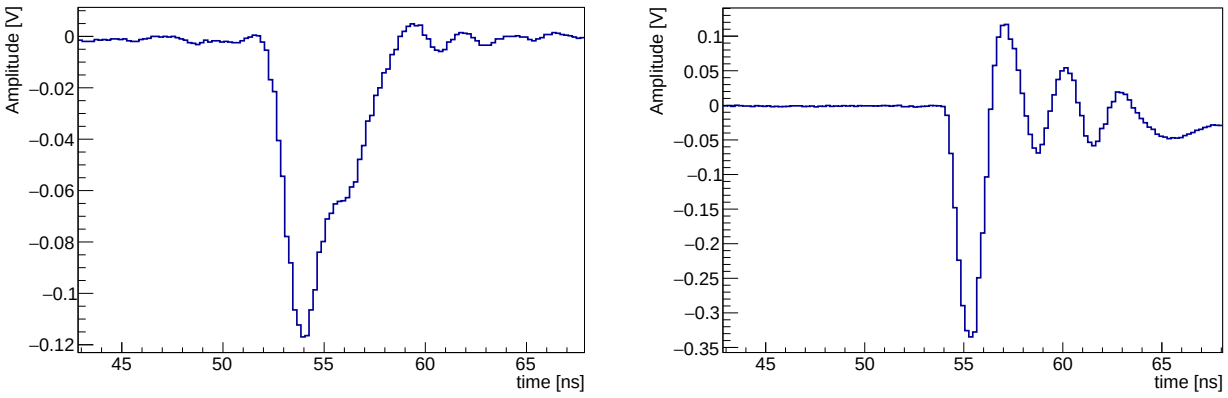

Figure 4: Examples of the signal pulse waveform for the silicon sensor (left) and the Photek MCP-PMT (right) digitized by CAEN V1742 digitizer board.

The raw waveforms are calibrated in both the voltage and time dimension using known inputs from a pulse generator [9]. The total collected charge for each signal pulse is computed by integrating a 10-ns window around the peak of the pulse. The time for the reference Photek MCP-PMT detector is obtained by fitting the peak region of the pulse to a Gaussian function and the mean parameter of the Gaussian is assigned as the timestamp. The time for signals from the silicon sensor is obtained by performed a linear fit to the rising edge of the pulse and the time at which the pulse reaches 30% of the maximum amplitude is assigned as its timestamp. We measured the electronic time resolution (TR) of the CAEN V1742 digitizer as ∼4 ps and neglected this impact on the timing measurements described below.

Electrons were identified using a combination of the gas Cherenkov counter provided by the FTBF and the signal size in the Photek detector located further downstream of the silicon sensor. Electromagnetic showers induced by electrons produce significantly larger signals in the Photek MCP-PMT, while pions produce a much smaller signal. After imposing the electron identification requirements the electron purity is between 80% and 90% for all beam conditions.

We begin by establishing the signal characteristics of a minimum-ionizing particle (MIP) using beams of 120 GeV protons as well as 8 GeV electrons with no absorbers upstream of the silicon pad sensor. To distinguish MIP signals from noise, we collect data events of pure noise with no beam and random triggers. The charge distribution for noise runs is presented in Fig. 5. As expected, the charge distribution for noise runs is centered at 0, and the RMS is about 2 fC.

In Figure 6, we show the response of the silicon sensor to the proton and electron beam without any absorbers upstream. We observe very similar response for these two cases, and measure an integrated charge of 4.5 fC and 5.0 fC for the proton and electron beams respectively. The measured charge takes into account the response of the amplifiers and attenuators used, which were measured in the lab using a pulse generator in the full dynamic range relevant for the current study. We expect that a MIP traversing a silicon sensor of thickness 300μm to produce roughly 32000 electron-hole

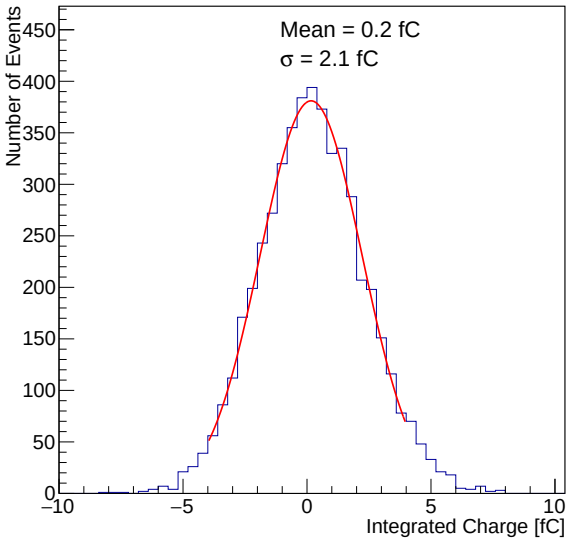

Figure 5: The distribution of charge integrated in the silicon sensor is shown for randomly triggered data recorded with no beam.

pairs, corresponding to a charge of about 5.1 fC. Thus, our measured value is in close agreement with expectations. Having established the absolute scale of the measured response using MIP's, in our remaining studies we normalize all charge measurements to the charge integrated in the silicon sensor for one MIP.

We study the response of the silicon sensor to electron beams of various energies after 6 radiation lengths of tungsten absorber. The silicon sensor is expected to be sensitive to the number of secondary electrons produced within the electromagnetic shower, and therefore its response is expected to scale up with higher incident electron energy. In Figure 7, we show an example of the integrated charge distribution measured in the silicon sensor after 6 radiation lengths of tungsten for 32 GeV electrons. We plot the mean and RMS of these distributions as a function of incident electron beam energy in Figure 8. The uncertainties plotted show the RMS of the charge distribution. We observe a fairly linear depedence between the measured charge and the incident beam energy, for beam energies between 4 GeV and 32 GeV.

In the Fig. 9 is shown longitudinal shower profile measured for 8 GeV electrons.

5 Discussion

Electric field applied to silicon results in the built-in junction voltage (0.6V) which is typical of silicon diodes. The high electric field in silicon leads to total depletion which is formed from a conducting region by removal of all free charge carriers. When charged particle pass through the totally depleted silicon region it produces carriers collecting on corresponding electrodes and producing output signal. Suppose the thickness of the silicon is 100 μm. The relativistic particle pass the 100 μm by 0.3 ps, so we can neglect this time (and jitter) in the consideration. The electrons produced by the particle collected on positive electrode and the holes on the negative. At high fields E ¿ 105 V/cm the mobility of carriers attain a constant drift velocity of 108 mm/s (1μm/10 ps) in the silicon [21]. The amount of electrons produced in the 100 um is 10000 (lets take this value instead of 8000 for simplicity). The time needed to collect all electrons in the 100 um is 1ns. The electrons produced closer to the positive electrode collected first. The time needed to pass 1 μm by electron is $\sim$10 ps. The average time between the electrons is $\sim$1 ps. If electronic can detect 100 electrons its arrival time could be inside of the 10 ps. The time jitter could be estimated

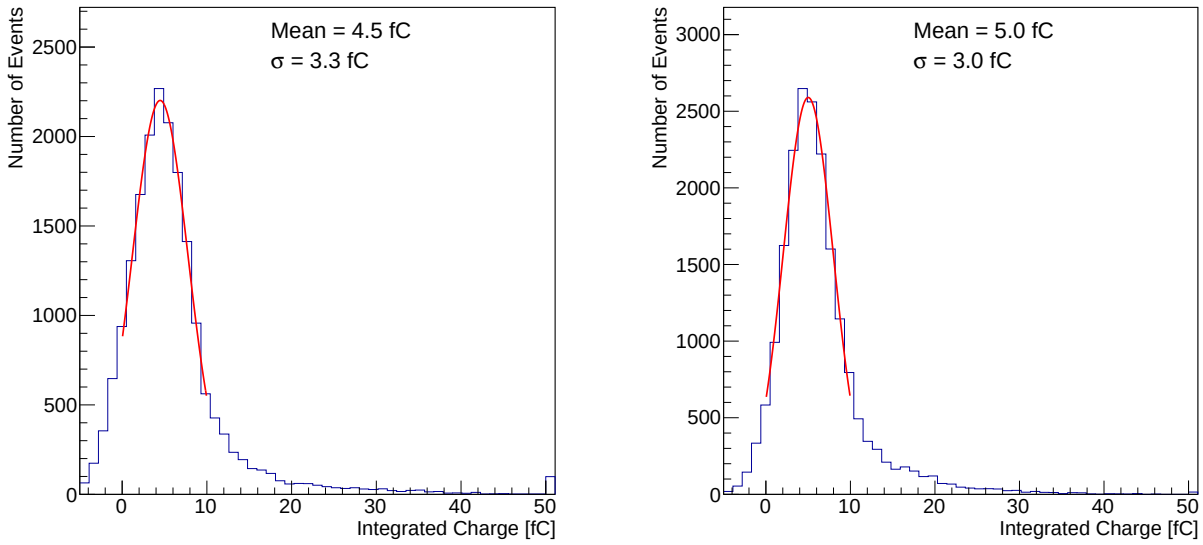

Figure 6: The distribution of charge integrated in the silicon sensor is shown for a beam of 120 GeV protons (left) and 8 GeV electrons (right) without any absorber upstream of the silicon sensor. These conditions mimic the response of the silicon sensor to a minimum-ionizing particle.

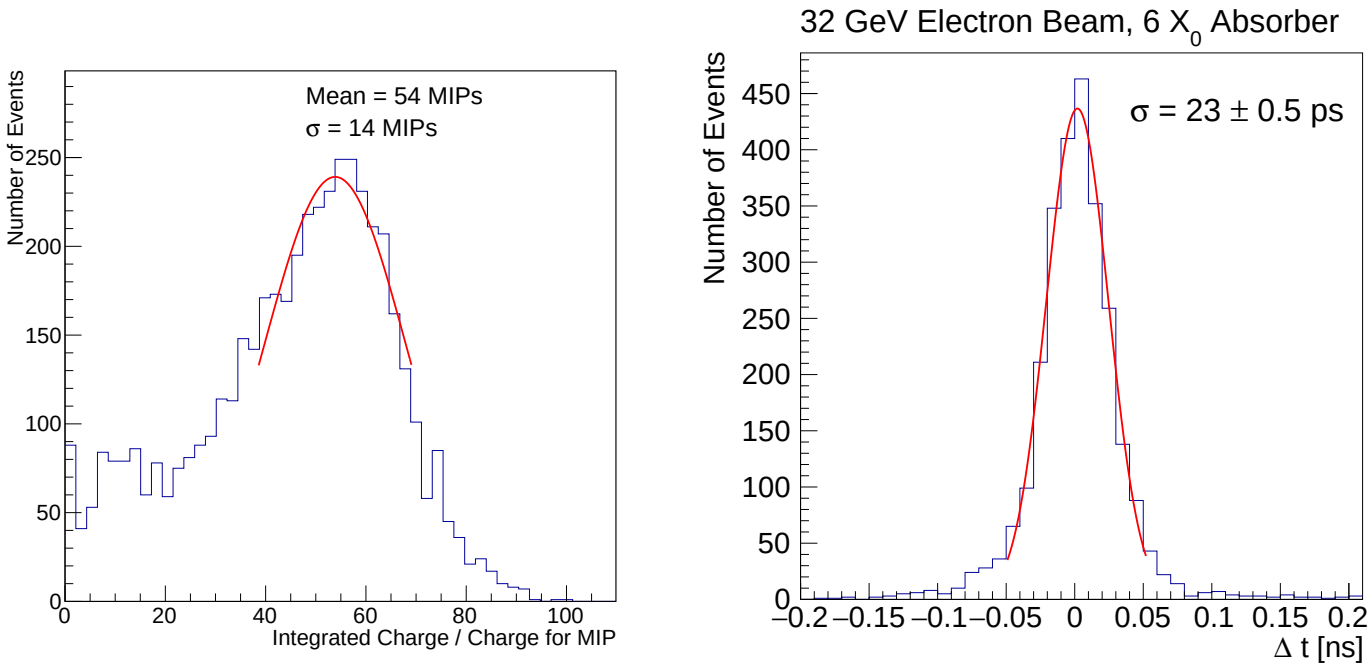

Figure 7: An example of the distribution of integrated charge in the silicon sensor is shown in units of the charge measured for MIP's. A 32 GeV electron beam is used, and the silicon sensor is placed after 6 radiation lengths of tungsten absorber.

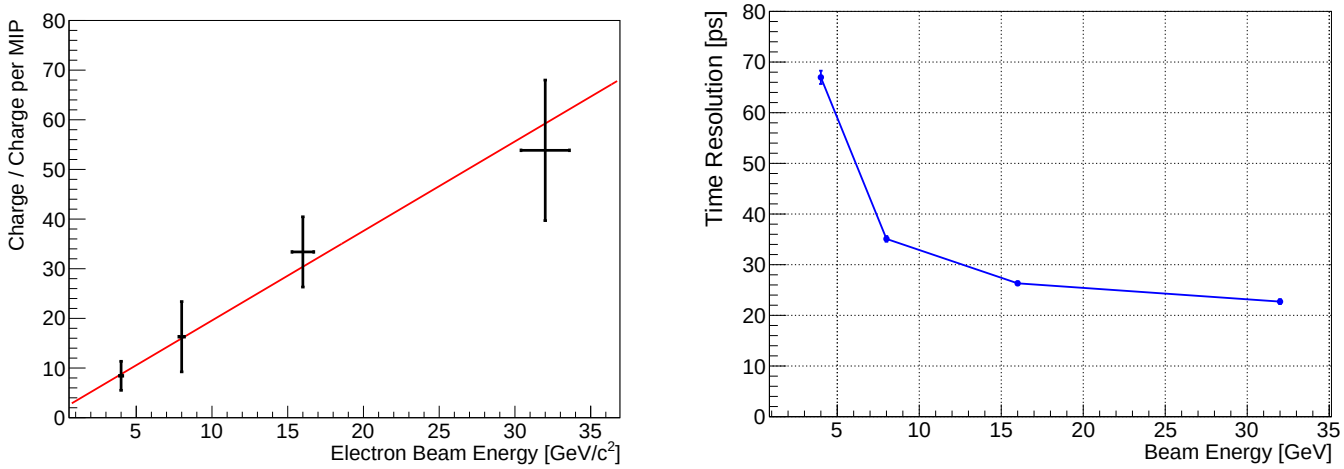

Figure 8: On the left, the integrated charge in the silicon sensor expressed in units of the charge measured for MIP's is shown as a function of the electron beam energy. The uncertainty bands show the RMS of the measured charge distribution. The red line is the best fit to a linear function. On the right, the measured time resolution between the silicon sensor and the Photek MCP-PMT reference is shown as a function of the electron beam energy.

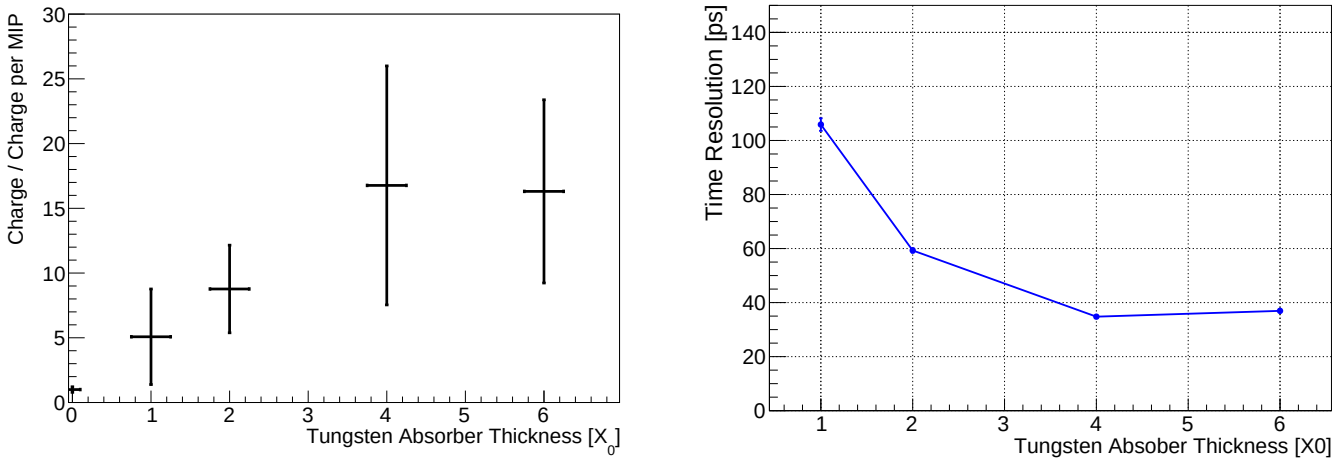

Figure 9: On the left, the integrated charge in the silicon sensor expressed in units of the charge measured for MIP's is shown as a function of the absorber (W) thickness measured in units of radiation lengths (X_0). The uncertainty bands show the RMS of the measured charge distribution. On the right, the time resolution between the silicon sensor and the Photek MCP-PMT reference is shown as a function of the absorber thickness.

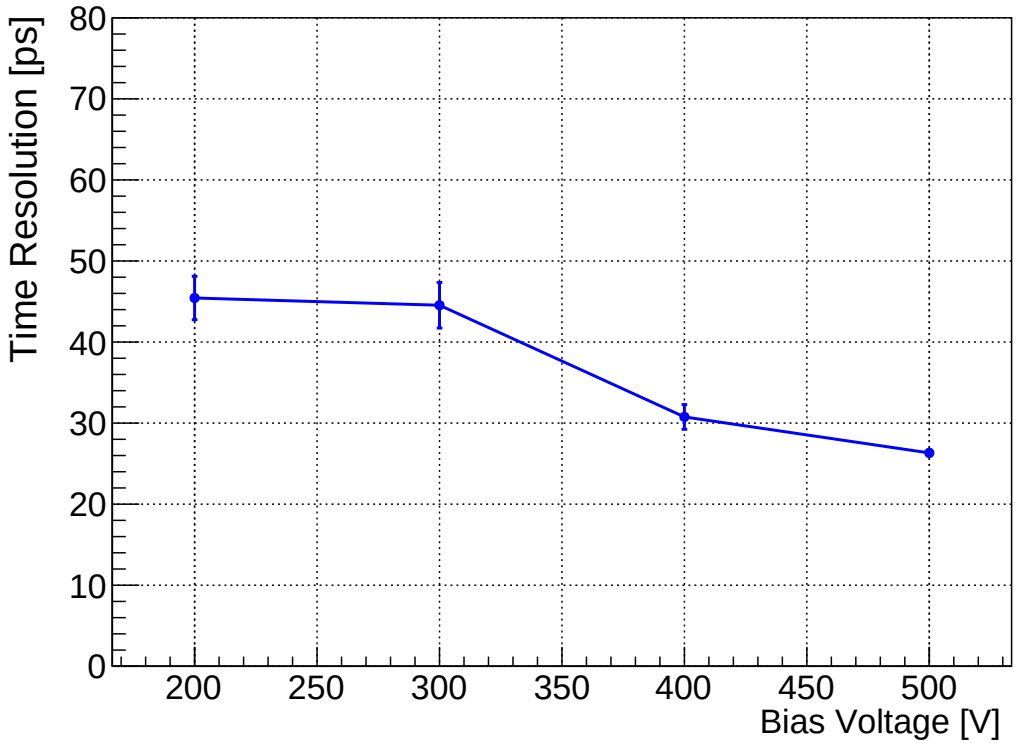

Figure 10: The time resolution between the silicon sensor and the Photek MCP-PMT reference is shown as a function of bias voltage applied on the silicon sensor.

as 3 ps for Poisson timing distribution. For example, if electronics can detects ∼100 electrons (with additional amplification) produced in silicon they collected from the thickness of ∼10 μm. We can say that the "rest of the silicon thickness" does not participate in the silicon time jitter, because these electrons are coming "too late". This simple model can explain in general obtained test beam results.The obtained data are in good consistency with calculation. The noise of the silicon with performed schematics is pretty low. It allows to detects the 120 GeV proton and 4 GeV electron (w/o absorber) with high efficiency, which could be estimated as $> 80\%$ (Figs. 6-8). The detected charge shows linear dependence on absorber length. (Figs. 9, 10). The longitudinal shower profile performed with the silicon is in good consistency with previous result obtained with MCP. The integrated silicon charge in dependence on Bias voltage show saturation at ∼500V for used silicon. This is $\sim$ 150 V less of maximum voltage that could be applied to the silicon. The measured and calculated time resolution for the silicon are in good consistency (Fig. 13).

6 Conclusion

We obtained time resolution for the silicon ∼23 ps. This could correspond to ∼137 particle registered in the shower. The 120 GeV proton amplitude corresponds to ∼20 mV according to measurements and estimation. We see significant amplitude increase when absorber used. This open an opportunity to use the silicon as active layer in calorimeter, for example in CMS HGC upgrade [22]. We can consider the results of this work as good opportunity to use silicon for timing measurements in future calorimeter. We plan to perform optimization of the possible silicon version, e.g. transverse size and configuration for multipixel readout, etc. This will be aim of our next work.

7 Acknowledgements

We thank FTBF personnel for very good beam condition during our test run. We also appreciate technical support of Fermilab SiDet department for production of high quality silicon samples. We appreciate Helmuth Spieler monography as a good source of silicon information [23].

References

[1] D. Anderson, A. Apresyan, A. Bornheim, J. Duarte, C. Pena, A. Ronzhin, M. Spiropulu, J. Trevor, and S. Xie, "On Timing Properties of LYSO-Based Calorimeters," *Nucl. Instrum. Meth.*, vol. A794, pp. 7–14, 2015.

[2] A. Ronzhin, S. Los, E. Ramberg, *et al.*, "Development of a new fast shower maximum detector based on microchannel plates photomultipliers (MCP-PMT) as an active element," *NIM* **A** *759 (2014) 65-73.*

[3] A. Ronzhin, S. Los, E. Ramberg, A. Apresyan, S. Xie, M. Spiropulu, and H. Kim, "Study of the timing performance of micro-channel plate photomultiplier for use as an active layer in a shower maximum detector," *Nuclear Instruments and Methods in Physics Research Section A: Accelerators, Spectrometers, Detectors and Associated Equipment*, vol. 795, pp. 288 – 292, 2015.

[4] A. Ronzhin, S. Los, E. Ramberg, A. Apresyan, S. Xie, M. Spiropulu, and H. Kim, "Direct tests of micro channel plates as the active element of a new shower maximum detector," *Nuclear Instruments and Methods in Physics Research Section A: Accelerators, Spectrometers, Detectors and Associated Equipment*, vol. 795, pp. 52 – 57, 2015.

[5] J. Butler, D. Contardo, M. Klute, J. Mans, and L. Silvestris, "Technical Proposal for the Phase-II Upgrade of the CMS Detector," Tech. Rep. CERN-LHCC-2015-010. LHCC-P-008, CERN, Geneva. Geneva, Jun 2015. Upgrade Project Leader Deputies: Lucia Silvestris (INFN-Bari), Jeremy Mans (University of Minnesota) Additional contacts: Lucia.Silvestris@cern.ch, Jeremy.Mans@cern.ch.

[6] D. Barney and M. Guthoff and A. Honma and S-W Li and A. Peisert and Y-M Tzeng and G Qin, "Measurement of the bulk leakage current of silicon sensors of the cms preshower after an integrated luminosity of 6.17 fb 1 , at s = 7 tev," *Journal of Instrumentation*, vol. 8, no. 02, p. P02004, 2013.

[7] `https://www.hamamatsu.com/resources/pdf/ssd/e10_handbook_for_high_energy.pdf`.

[8] `http://www.caen.it/csite/CaenProd.jsp?parent=11&idmod=661`.

[9] H. Kim, C.-T. Chen, N. Eclov, A. Ronzhin, P. Murat, E. Ramberg, S. Los, W. Moses, W.-S. Choong, and C.-M. Kao, "A new time calibration method for switched-capacitor-array-based waveform samplers," *Nuclear Instruments and Methods in Physics Research Section A: Accelerators, Spectrometers, Detectors and Associated Equipment*, vol. 767, pp. 67 – 74, 2014.